Nanostructures

DOI: 10.1002/ange.201407387

Size-Controlled Synthesis of Conjugated Polymer Nanoparticles in Confined Nanoreactors**

Sheng Deng, Jian Zhi, Xianmei Zhang, Qingqing Wu, Yun Ding, and Aiguo Hu**

Abstract: *Soluble conjugated polymeric nanoparticles are synthesized by Suzuki-type polycondensation of two monomers ($A_x + B_y$, $x > 2$, $y \geq 2$) in the channel of ordered mesoporous silica-supported carbon nanomembranes (nanoreactors). These synthesized soluble conjugated microporous polymers (SCMPs) exhibit uniform particle-size distributions and well-controlled particle sizes. The control of particle size stems from the fact that the polycondensations exclusively take place inside the mesochannels of the nanoreactors. Photoluminescence studies show that polymeric nanoparticles with tetraphenylethene and pyrene substructures are highly fluorescent. The combination of both physical stability and processability offered by the soluble polymeric nanoparticles makes them particularly attractive in light emitting and other optoelectronic applications.*

Condensation polymerization is an important class of polymerization where monomers bearing two or more reactive end groups join together. Linear polymers are created when both monomers have two end groups ($A_2 + B_2$), while one or more monomers with more than two end groups ($A_x + B_y$, $x > 2$, $y \geq 2$) will generate three-dimensional polymers which are typically crosslinked. The latter is widely used in the preparation of conjugated microporous polymers (CMPs).[1] In recent years, CMPs with both π-conjugated skeletons and permanent nanopores have emerged as an important material platform. They have shown potential applications in gas adsorption,[1a,g,2] electrical energy storage,[3] light emitting,[1f] and heterogeneous catalysis.[1j,4] Most of these materials are however insoluble regardless of the solvent used. The insolubility limits the further application of the CMPs in more interesting fields, where the combination of the unique features of CMPs, like porosity, conjugation, and optical property could be taken advantage of. Indeed, processability and device integration have been described as among the three most important advances needed for CMPs to be competitive in future applications.[5] Meanwhile, the generation of sub-10 nm conjugated polymer particles was considered a prospective target.[6]

Many research efforts have been focused on solving the solubility issue of CMPs. Soluble hyperbranched polyphenylenes were synthesized with an AB_2-type monomer.[7] Soluble dendritic pyrenes were prepared by using a generation-by-generation technique.[8] Unfortunately, specially designed monomers and/or tedious synthetic procedures are required in these approaches. To date, the synthesis of CMPs with variable structural features and functionalities still constitutes a great challenge. The closest steps towards the fabrication of soluble CMPs have been reprecipitation methods[6,9] and emulsion techniques,[10] thus leading to solution-dispersible nanoparticles. Recently, Cooper et al.[11] reported the first example of soluble CMPs (SCMPs) through hyperbranching of a tetrasubstituted pyrene monomer (A_4) in the presence of a disubstituted pyrene monomer, which was introduced to limit the molecular weight of the SCMPs.

Herein we report a new method to synthesize size-controlled SCMPs. The synthesis is based on mesopore-confined growth of CMPs. Therefore, limiting the polycondensation taking place exclusively inside the mesoporous reactors is essential for this strategy. Initially, we focused on the Suzuki-type polycondensation between an A_3 monomer, 1,3,5-triiodobenzene (**1**), and a B_2 monomer, 1,4-phenylenediboronic acid (**2**). Direct mixing of these two monomers in the presence of a homogenous palladium catalyst (e.g., $[Pd(PPh_3)_2Cl_2]$) resulted in the formation of insoluble three-dimensional networks, and is similar to the synthesis of the insoluble CMPs. To limit the polymer growth in a confined space, we embedded the catalyst (palladium nanoparticles) in mesoporous supports, namely, silica-supported carbon nanomembranes (SS-CNMs). The SS-CNMs were prepared by formation of self-assembled monolayers of enediyne compounds on the surface of mesoporous silicas followed by thermally triggered Bergman cyclization and carbonization.[12]

In this study, three SS-CNMs (denoted as SS-CNM-1, SS-CNM-2 and SS-CNM-3) were chosen as nanoreactors for catalyst impregnation. They were prepared from mesoporous silicas with the same space group (*P*6mm) and with pore sizes

[*] S. Deng, Dr. J. Zhi, X. Zhang, Q. Wu, Prof. A. Hu
Shanghai Key Laboratory of Advanced Polymeric Materials
School of Materials Science and Engineering
East China University of Science and Technology
Shanghai, 200237 (China)
E-mail: hagmhsn@ecust.edu.cn
Dr. Y. Ding
Department of Chemistry and Applied Biosciences
Eidgenössische Technische Hochschule Zurich and Facoltà di Informatica, Instituto di Scienze Computationali
Università della Svizzera Italiana
CH-6900 Lugano (Switzerland)
E-mail: yun.ding@phys.chem.ethz.ch

[**] The support of the National Natural Science Foundation of China (20874026, 91023008), Ph.D. Programs Foundation of Ministry of Education of China (20100074110002), the Fundamental Research Funds for the Central Universities, and Shanghai Leading Academic Discipline Project (B502) is gratefully acknowledged. A.H. thanks the "Eastern Scholar Professorship" support from Shanghai local government and Prof. Baohang Han for providing several key monomers.

Supporting information for this article is available on the WWW under http://dx.doi.org/10.1002/anie.201407397.

ranging from small (MCM-41), to middle (SBA-15), to large (pore expanded SBA-15). The pore sizes of these three nanoreactors are 3.4, 5.4, and 7.2 nm, respectively (see Table S1 in the Supporting Information), and are slightly smaller than those of the mesoporous silicas because of the formation of the carbon nanomembrane on the internal surface of the mesopores. To achieve a uniform distribution of the palladium nanoparticles inside the mesochannels of the nanoreactors, a freeze-drying technique[13] was exploited. The palladium nanoparticles settled on the external surface of the nanoreactors were carefully washed away with cold aqua regia. Figure 1 shows the transmission electron microscopy

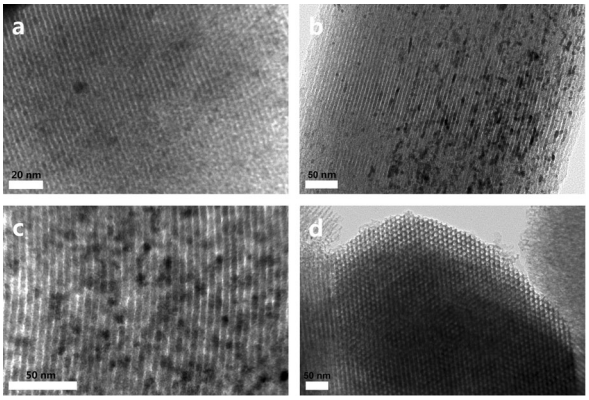

Figure 1. TEM images of Pd@SS-CNM-1 (a), Pd@SS-CNM-2 (b), and Pd@SS-CNM-3 (c and d).

(TEM) images of the three Pd@SS-CNM catalysts. The lattice fringes and the hexagonal structure of the nanoreactors are maintained after the embedding the palladium nanoparticles. All the palladium nanoparticles are well dispersed inside the mesochannels. No palladium nanoparticle is found outside of the nanoreactors, which is essential for the confined growth of the CMPs.

The polycondensations between the monomers **1** and **2** were performed in *N*,*N*-dimethylformamide (DMF) with Pd@SS-CNMs as catalysts and tetrabutylammonium fluoride (TBAF) as the base (Scheme 1). After purification by

Scheme 1. Size-controlled synthesis of SCMPs in a nanoreactor.

sequential Soxhlet extraction, the polymers (SCMP1–SCMP3) were isolated as colorless films. Further precipitation in an antisolvent gave the polymers as off-white powders (Figure 2a). Scanning electron microscopy (SEM) images reveal that the powders comprise fused spheres of 500–1000 nm in diameter (Figure 2c). These polymers are freely soluble in a variety of organic solvents, like dichloromethane,

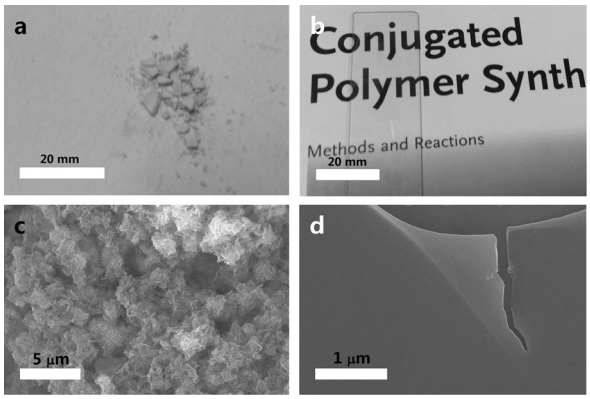

Figure 2. a) Photograph of antisolvent-precipitated SCMP2 powder. b) Photograph of solvent-cast film of SCMP2 on a glass slide. c) SEM image of the antisolvent-precipitated SCMP2 powder. d) SEM image of the solvent-cast SCMP2 film.

ethyl acetate, tetrahydrofuran, toluene, and DMF to give colorless transparent solutions (see Figure S1B). The solutions are subjected to solvent-casting to form transparent films (Figure 2b). SEM images show that all the solvent-cast films have smooth and uniform surfaces (Figure 2d).

Figure 3 and Table 1 show the particle size and size distribution of these SCMPs obtained using a Zetasizer Nano (Malvern, UK) at 25 °C. Narrow size distributions and average particle sizes of 2.4, 3.8, and 5.4 nm are found for SCMP1, SCMP2, and SCMP3, respectively. It is noteworthy that the sizes of SCMPs are only slightly smaller than the pore

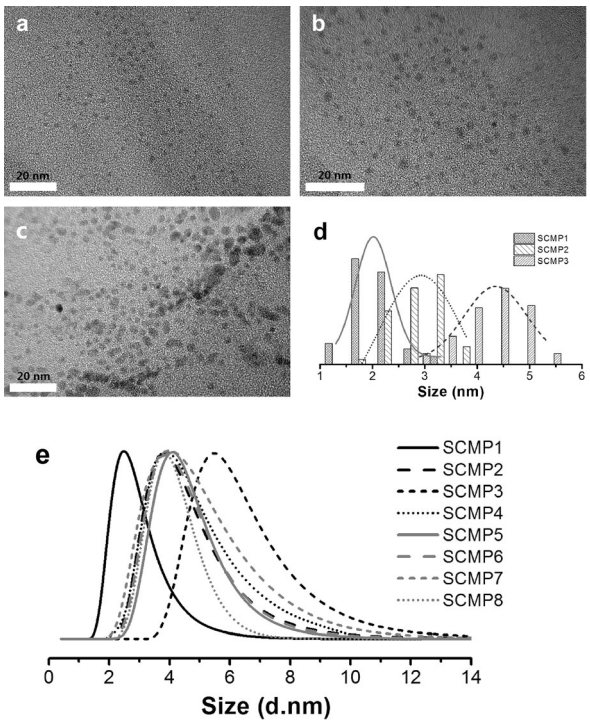

Figure 3. HR-TEM images of SCMP1 (a), SCMP2 (b), and SCMP3 (c). d) Size histogram of three SCMPs obtained with HR-TEM. e) Normalized size distributions of all the SCMPs in DMF obtained with DLS.

Table 1: Particle sizes of polymer nanoparticles SCMP1–SCMP8.

	Pore size [nm][a]	A_x monomer	B_y monomer	DLS [nm][b]
SCMP1	3.4	**1**	**2**	2.4
SCMP2	5.4	**1**	**2**	3.8
SCMP3	7.2	**1**	**2**	5.4
SCMP4	5.4	**1**	**3**	4.0
SCMP5	5.4	**4**	**2**	4.1
SCMP6	5.4	**5**	**2**	3.9
SCMP7	5.4	**5**	**3**	4.0
SCMP8	5.4	**6**	**2**	3.8

[a] Pore sizes of nanoreactors were determined through nitrogen adsorption analysis. [b] Sizes of polymer nanoparticles were measured using DLS.

sizes of the nanoreactors, thus implying that the sizes of SCMPs are controlled by the pore sizes of the nanoreactors because the polycondensations take place exclusively inside the confined pores of SS-CNM nanoreactors. The SCMP nanoparticles are also visualized with high-resolution TEM (HR-TEM) (Figure 3a–c). Uniformly distributed particles with sizes from small to large (SCMP1 to SCMP3) were clearly observed. The sizes measured with HR-TEM are consistent with those obtained from dynamitic light scattering (DLS) analysis. GPC analysis on the three SCMPs revealed narrowly dispersed molecular weights from low to high (see Figure S2). The molecular weights obtained from GPC might be underestimated as these nanoparticles are structurally more compact than the polystyrene standards.[11] To figure out the most probable structures corresponding to SCMP1–SCMP3, theoretical simulations are carried out based on a model dendrimer structure from generation 2 to generation 4.5, where only H atoms are present at the termini. The calculated sizes of generation 2, 3, and 4 dendrimers match quite well with the experimental values of SCMP1, SCMP2, and SCMP3, respectively (see Table S2).

The ^{1}H NMR spectra of the SCMPs are similar to that of the model compound 1,3,5-triphenylbenzene (see Figure S3), where the majority of the peaks appear between $\delta = 7.0$–7.7 ppm. The presence of the iodine and boronic acid terminal groups was confirmed by derivatization of these SCMPs. Briefly, the as-prepared SCMPs were first treated with an excess of 4-methoxyphenylboronic acid, and after that, treated with 4-iodotoluene (large excess compare to 4-methoxyphenylboronic acid) for 8 hours, in the presence of a homogeneous catalyst $[Pd(PPh_3)_2Cl_2]$. After purification with column chromatography, the SCMP derivatives show two peaks corresponding to the methoxy group ($\delta =$ 3.74 ppm) and the methyl group ($\delta = 2.28$ ppm) in the ^{1}H NMR spectrum (see Figure S4). The ratio between the iodine and the boronic acid termini on the original SCMP was thus calculated based on the integration ratio of these two peaks. The results show that more iodine atoms are present than boronic acid groups on SCMPs, with the ratio around 4.65:1. It is well acknowledged that the oxidative addition of an aryl halide to a palladium(0) species is typically the rate-determining step in a cross-coupling reaction.[14] Theoretically, it is more difficult for the iodo groups on a giant SCMP particle to diffuse to the palladium nanoparticle than those small molecular aryl iodides (which eventually react with the boronic acid groups on the SCMP particles). Therefore, more iodo groups were left on the SCMP particles.

To ascertain that the polycondensations are accessing the internal palladium nanoparticles through the open channels, we used the as-synthesized SCMPs of varying sizes as probes. An orthogonal experiment was designed to check the relative reactivity of these SCMPs with iodobenzene in these nanoreactors. A heterogeneous catalyst with palladium nanoparticles on both the external and internal surface of SS-CNM-3 (Pd/SS-CNM-3)[15] was also used as a control. The consumption of iodobenzene was monitored with gas chromatography (GC). In all cases, the consumption of iodobenzene reaches a plateau in less than 10 hours with Pd/SS-CNM-3 as the catalyst. In contrast, the same reaction takes place much more slowly in all Pd@SS-CNMs, thus indicating that the access of the SCMP nanoparticles to the internal palladium catalysts is more difficult than to those on the external surface. Table 2 shows the normalized consumption

Table 2: Normalized consumption of iodobenzene when reacted with SCMPs in the presence of different catalysts.

	SCMP1 [%]	SCMP2 [%]	SCMP3 [%]
Pd/SS-CNM[a]	100	71	35
Pd@SS-CNM-3	54	33	6
Pd@SS-CNM-2	38	4	1
Pd@SS-CNM-1	3	0	0

[a] Palladium nanoparticles were loaded on both external and internal surfaces of SS-CNM-3.

percentage of iodobenzene. The number drops gradually as the size of SCMP particles used increases, thus implying the lower contents of termini groups on the larger SCMP particles. More interestingly, the smallest SCMPs (SCMP1) can diffuse into the mesochannels of larger nanoreactors (SS-CNM-2 and SS-CNM-3) to give considerable derivatization degrees with iodobenzene. In contrast, the middle-sized SCMP nanoparticles can only enter the largest nanoreactors, while the largest SCMP nanoparticles can hardly enter either nanoreactor, thus leading to negligible consumption of iodobenzene. This set of experiments unambiguously demonstrates that the polycondensation is a true confined growth with the monomers accessing the palladium nanoparticles through the open channels.

The Suzuki-type polycondensation in the nanoreactors were further explored by using different types of monomers, like 4,4′-biphenydiboronic acid (**3**), tetrakis(4-bromophenyl)-methane (**4**), 1,3,6,8-tetrabromopyrene (**5**), and 1,1,2,2-tetrakis(4-bromophenyl)ethane (**6**). All the SCMPs obtained are fine powders. They are freely soluble in common organic solvents. After solvent casting on a glass slide, all the SCMPs form transparent films with smooth and uniform surfaces as revealed by SEM (see Figures S1B and C). Interestingly, the sizes of different kinds of SCMPs (SCMP2 and SCMP4–SCMP8) are exactly the same when the polycondensations are conducted in the nanoreactor of the same pore size (Figure 3e), thus corroborating the size-controlled growth of SCMP nanoparticles in the nanoreactors.

The UV/Vis spectra (see Figure S7) of all eight SCMPs are similar to each other, thus showing the main absorption around $\lambda = 275$ nm, which is attributed to the π–π^* transition of the aryl units. The photoluminescence (PL) spectra (see Figure S8) of SCMP1–SCMP5 show emission maximum at $\lambda = 350$ nm, similar to that of the model compound 1,3,5-triphenylbenzene. The emission peak of SCMP5 tails up to $\lambda = 500$ nm, thus showing visible florescence when irradiated with a UV ($\lambda = 365$ nm) light (Figure 4). The SCMP6 shows

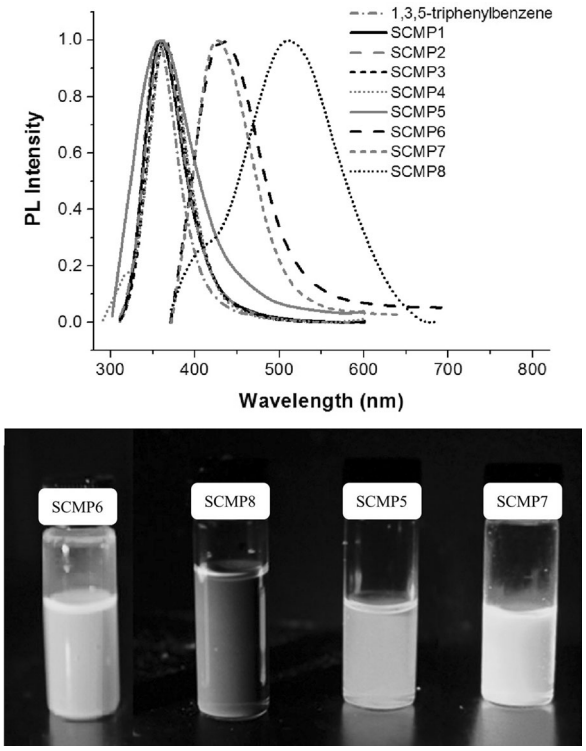

Figure 4. a) Normalized fluorescence spectra of SCMP1–SCMP8 and the model compound 1,3,5-triphenylbenzene. b) Solutions of SCMP5–SCMP8 in THF show bright luminescence under UV irradiation ($\lambda = 365$ nm).

fluorescence with an emission maximum at $\lambda = 433$ nm, while the fluorescence of the SCMP7 shows a blue shift to $\lambda =$ 425 nm as benzene ring is flexible enough to turn out of the conjugation plane and thus disturbs the conjugated system.[1c] With the increasing incorporation of benzene rings into the pyrene units, the emission maximum shifts to shorter wavelengths. The quantum yields of the SCMP6 and SCMP7 were calculated to be 37 and 53%, respectively, relative to that of quinine sulfate (excited at $\lambda = 350$ nm). Both SCMP6 and SCMP7, having pyrene units, are highly luminescent conjugated polymers thanks to the restricted rotation of the polymer building blocks. The tetraphenylethene units are known to only show weak fluorescence in solution.[16] Interestingly, when this unit was incorporated into the SCMP network, the rotation of phenyl units was restricted by the formation of a three-dimensional network, thus promoting π-electronic conjugation, facilitating long-range exciton migration, and hence enhancing the luminescence efficiency. The SCMP8 showed bright green luminescence when excited with UV light (Figure 4).

In summary, by embedding the catalyst (palladium nanoparticles) in the channel of mesoporous silica-supported carbon nanomembranes (SS-CNMs), structurally well-defined nanoreactors are generated. The Suzuki-type polycondensation between monomers ($A_x + B_y$, $x > 2$, $y \geq 2$) takes place inside the mesopore of the nanoreactor exclusively. The growth of the CMP nanoparticles ceases when their sizes are comparable to that of the nanoreactor, thus leading to the size-controlled synthesis of SCMPs. The combination of physical stability and processability offered by SCMPs makes them particularly attractive in polymer light emitting diodes (PLEDs) and polymer solar cells. This catalyst@pore strategy can also be generally appreciated in the synthesis of other types of soluble hyperbranched polymers in a simple but controllable manner.

Experimental Section

Synthesis of SCMP2:

1) Polycondensation: 1,3,5-Triiodobenzene (0.114 g, 0.25 mmol), *p*-phenylenediboronic acid (0.062 g, 0.375 mmol), TBAF (0.710 g, 2.25 mmol), Pd@SS-CNM-2 (2.5 mg, 1.1×10^{-3} mmol of Pd), and DMF (5 mL) were successively added to a 25 mL sealed tube under a nitrogen atmosphere. After degassed by three freeze-pump-thaw cycles, the mixture was sealed and stirred at 80 °C for 120 h.

2) Termination: The above mixture was cooled to room temperature, and then transferred to a 50 mL Schlenk flask. $[Pd(PPh_3)_2Cl_2]$ (16 mg, 0.021 mmol), 2 M K_2CO_3 in water (5 mL), phenylboronic acid (92 mg, 0.75 mmol), and DMF (15 mL) were added successively followed by three freeze–pump–thaw cycles. The mixture was stirred at 80 °C for 12 h. After cooling to room temperature, iodobenzene (0.5 mL, 4.46 mmol), and $[Pd(PPh_3)_2Cl_2]$ (16 mg, 0.021 mmol) were added and the solution was degassed. The mixture was then heated to 80 °C and stirred for 12 h under a nitrogen atmosphere.

3) Purification: The resulting light green mixture was neutralized with dilute hydrochloric acid, and then diluted with dichloromethane (100 mL), washed with saturated Na_2HPO_4 solution (3×100 mL), followed by deionized water (3×100 mL) and dried over $MgSO_4$. The clear solution was concentrated at reduced pressure, and then added with silica gel (3 g) and dried under vacuum at room temperature. The silica adsorbed product was Soxhlet extracted for 24 h with petroleum ether, water, and THF. The THF extraction was evaporated under vacuum for 12 h at 110 °C to gain product as viscous solid (41 mg, 87%).

The reason that $[Pd(PPh_3)_2Cl_2]$ was used in the termination step is that it was impossible to cap all the terminal boronic acid and iodine functionality in the original system because of the fact that it is difficult for the giant polymeric nanoparticles to diffuse into the mesochannel to meet with the palladium catalysts. Therefore, the homogenous catalyst is added.

The polymeric product may also be separated without termination. After the first step, the polymeric product was obtained by precipitation in an anti-solvent (methanol).

Received: July 19, 2014
Revised: August 28, 2014
Published online: October 15, 2014

Keywords: conjugation · electron microscopy · nanoparticles · palladium · polymers

[1] a) Q. Chen, J.-X. Wang, Q. Wang, N. Bian, Z.-H. Li, C.-G. Yan, B.-H. Han, *Macromolecules* **2011**, *44*, 7987 – 7993; b) L. Chen, Y. Yang, D. Jiang, *J. Am. Chem. Soc.* **2010**, *132*, 9138 – 9143; c) J. Schmidt, M. Werner, A. Thomas, *Macromolecules* **2009**, *42*, 4426 – 4429; d) J. X. Jiang, A. Cooper, *Angew. Chem. Int. Ed.* **2007**, *46*, 8574 – 8578; *Angew. Chem.* **2007**, *119*, 8728 – 8732; e) J.-X. Jiang, F. Su, A. Trewin, C. Wood, H. Niu, J. Jones, Y. Khimyak, A. Cooper, *J. Am. Chem. Soc.* **2008**, *130*, 7710 – 7720; f) L. Chen, Y. Honsho, S. Seki, D. Jiang, *J. Am. Chem. Soc.* **2010**, *132*, 6742 – 6748; g) K. V. Rao, *J. Mater. Chem.* **2011**, *21*, 12958 – 12963; h) Y. Xu, L. Chen, Z. Guo, A. Nagai, D. Jiang, *J. Am. Chem. Soc.* **2011**, *133*, 17622 – 17625; i) Z. Chang, D.-S. Zhang, Q. Chen, X.-H. Bu, *Phys. Chem. Chem. Phys.* **2013**, *15*, 5430 – 5442; j) Y. Xu, S. Jin, H. Xu, A. Nagai, D. Jiang, *Chem. Soc. Rev.* **2013**, *42*, 8012 – 8031; k) A. Thomas, *Angew. Chem. Int. Ed.* **2010**, *49*, 8328 – 8344; *Angew. Chem.* **2010**, *122*, 8506 – 8523.

[2] a) P. Kuhn, A. L. Forget, D. Su, A. Thomas, M. Antonietti, *J. Am. Chem. Soc.* **2008**, *130*, 13333 – 13337; b) X. Liu, Y. Xu, D. Jiang, *J. Am. Chem. Soc.* **2012**, *134*, 8738 – 8741; c) M. Rose, *Soft Matter* **2010**, *6*, 3918 – 3923.

[3] Y. Kou, Y. Xu, Z. Guo, D. Jiang, *Angew. Chem. Int. Ed.* **2011**, *50*, 8753 – 8757; *Angew. Chem.* **2011**, *123*, 8912 – 8916.

[4] a) J. Schmidt, J. Weber, J. D. Epping, M. Antonietti, A. Thomas, *Adv. Mater.* **2009**, *21*, 702 – 705; b) J.-X. Jiang, C. Wang, A. Laybourn, T. Hasell, R. Clowes, Y. Z. Khimyak, J. Xiao, S. J. Higgins, D. J. Adams, A. I. Cooper, *Angew. Chem. Int. Ed.* **2011**, *50*, 1072 – 1075; *Angew. Chem.* **2011**, *123*, 1104 – 1107; c) Z. Xie, C. Wang, K. deKrafft, W. Lin, *J. Am. Chem. Soc.* **2011**, *133*, 2056 – 2059.

[5] F. Vilela, K. Zhang, M. Antonietti, *Energy Environ. Sci.* **2012**, *5*, 7819 – 7832.

[6] J. Pecher, S. Mecking, *Chem. Rev.* **2010**, *110*, 6260 – 6279.

[7] a) H. K. Young, W. W. Owen, *J. Am. Chem. Soc.* **1990**, *112*, 4592 – 4593; b) Y. H. Kim, O. W. Webster, *Macromolecules* **1992**, *25*, 5561 – 5572.

[8] T. M. Figueira-Duarte, S. C. Simon, M. Wagner, S. I. Druzhinin, K. A. Zachariasse, K. Müllen, *Angew. Chem. Int. Ed.* **2008**, *47*, 10175 – 10178; *Angew. Chem.* **2008**, *120*, 10329 – 10332.

[9] a) D. Tuncel, H. V. Demir, *Nanoscale* **2010**, *2*, 484 – 494; b) C. Wu, C. Szymanski, Z. Cain, J. McNeill, *J. Am. Chem. Soc.* **2007**, *129*, 12904 – 12905; c) C. Wu, J. McNeill, *Langmuir* **2008**, *24*, 5855 – 5861; d) N. A. A. Rahim, W. McDaniel, K. Bardon, S. Srinivasan, V. Vickerman, P. T. C. So, J. H. Moon, *Adv. Mater.* **2009**, *21*, 3492 – 3496; e) L. Feng, L. Liu, F. Lv, G. C. Bazan, S. Wang, *Adv. Mater.* **2014**, *26*, 3926 – 3930.

[10] a) P. Zhang, Z. Weng, J. Guo, C. Wang, *Chem. Mater.* **2011**, *23*, 5243 – 5249; b) A. Berkefeld, S. Mecking, *Angew. Chem. Int. Ed.* **2006**, *45*, 6044 – 6046; *Angew. Chem.* **2006**, *118*, 6190 – 6193; c) M. C. Baier, J. Huber, S. Mecking, *J. Am. Chem. Soc.* **2009**, *131*, 14267 – 14273; d) H. Li, X. Wu, B. Xu, H. Tong, L. Wang, *RSC Adv.* **2013**, *3*, 8645 – 8648.

[11] G. Cheng, T. Hasell, A. Trewin, D. Adams, A. Cooper, *Angew. Chem. Int. Ed.* **2012**, *51*, 12727 – 12731; *Angew. Chem.* **2012**, *124*, 12899 – 12903.

[12] X. Yang, Z. Li, J. Zhi, J. Ma, A. Hu, *Langmuir* **2010**, *26*, 11244 – 11248.

[13] T. M. Eggenhuisen, H. Friedrich, F. Nudelman, J. Zečević, N. A. J. M. Sommerdijk, P. E. de Jongh, K. P. de Jong, *Chem. Mater.* **2013**, *25*, 890 – 896.

[14] L. X. Yin, J. Liebscher, *Chem. Rev.* **2007**, *107*, 133 – 173.

[15] J. Zhi, D. Song, Z. Li, X. Lei, A. Hu, *Chem. Commun.* **2011**, *47*, 10707 – 10709.

[16] W. B. Wu, S. H. Ye, G. Yu, Y. Q. Liu, J. G. Qin, Z. Li, *Macromol. Rapid Commun.* **2012**, *33*, 164 – 171.

